The antiapoptotic protein HAX-1 mediates half of phospholamban's inhibitory activity on calcium cycling and contractility in the heart

Received for publication, September 27, 2017, and in revised form, November 17, 2017 Published, Papers in Press, November 17, 2017, DOI 10.1074/jbc.RA117.000128

Philip A. Bidwell[‡], **Kobra Haghighi**[‡], **and Evangelia G. Kranias**[‡§1]

From the [‡]*Department of Pharmacology and Systems Physiology, University of Cincinnati College of Medicine, Cincinnati, Ohio 45267 and the* [§]*Department of Molecular Biology, Center of Basic Research, Biomedical Research Foundation, Academy of Athens, 115 27 Athens, Greece*

Edited by Roger J. Colbran

The antiapoptotic protein HAX-1 (HS-associated protein X-1) localizes to sarcoplasmic reticulum (SR) in the heart and interacts with the small membrane protein phospholamban (PLN), inhibiting the cardiac sarco/endoplasmic reticulum calcium ATPase 2a (SERCA2a) in the regulation of overall calcium handling and heart muscle contractility. However, because global HAX-1 deletion causes early lethality, how much endogenous HAX-1 contributes to PLN's inhibitory activity on calcium cycling is unknown. We therefore generated a cardiac-specific and inducible knock-out mouse model. HAX-1 ablation in the adult heart significantly increased contractile parameters and calcium kinetics, associated with increased SR calcium load. These changes occurred without any changes in the protein expression of SERCA2a, PLN, and ryanodine receptor or in the PLN phosphorylation status. The enhanced calcium cycling in the HAX-1–depleted heart was mediated through increases in the calcium affinity of SERCA2a and reduced PLN–SERCA2a binding. Comparison of the HAX-1 deletion–induced stimulatory effects with those elicited by PLN ablation indicated that HAX-1 mediates ~50% of the PLN-associated inhibitory effects in the heart. Stimulation with the inotropic and lusitropic agent isoproterenol eliminated the differences among wild-type, HAX-1–deficient, and PLN–deficient hearts, and maximally stimulated contractile and calcium kinetic parameters were similar among these three groups. Furthermore, PLN overexpression in the HAX-1–null cardiomyocytes did not elicit any inhibitory effects, indicating that HAX-1 may limit PLN activity. These findings suggest that HAX-1 is a major mediator of PLN's inhibitory activity and a critical gatekeeper of SR calcium cycling and contractility in the heart.

Depressed sarcoplasmic reticulum (SR)[2] calcium transport, associated with impaired cardiomyocyte calcium cycling and contractility, is a major characteristic of human and experimental heart failure (1, 2). SR Ca^{2+} transport is mediated by the cardiac isoform of the sarco/endoplasmic reticulum Ca^{2+}-ATPase 2a (SERCA2a), which is one of the most abundant proteins in the heart. SERCA2a is regulated by a small integral membrane, phospholamban (PLN), phosphorylation of which during fight-or-flight responses relieves its inhibitory effects, enhancing cardiac function (3). Over the last several decades, PLN and SERCA2a have been characterized in great detail by an abundance of biochemical and biophysical studies (3). An elegant structure–function model has been generated in which PLN stabilizes a conformation of SERCA2a with a low Ca^{2+} affinity, thus decreasing enzymatic activity (4). From the physiological perspective, the role of PLN in cardiac function has been elucidated by the generation and characterization of genetically altered mouse models. Ablation of PLN was associated with enhanced Ca^{2+} cycling and contractile parameters, resulting in an overall hypercontractile cardiac function (5, 6), which persisted throughout aging (7). In contrast, overexpression of PLN in the heart resulted in depressed calcium kinetics and contractile parameters, but the inhibitory effects were relieved upon PLN phosphorylation by β-adrenergic agonists (8, 9). However, accumulating evidence indicates that regulation of SR Ca^{2+}-transport is more complicated than we originally perceived, and there are several proteins that physically interact with PLN and may modulate cardiomyocyte Ca^{2+} handling (1, 10). One of these proteins is HAX-1 (HS-associated protein X-1), which has been found to directly interact with PLN (11) and modulate its activity (13).

HAX-1 is an ~35-kDa protein that is ubiquitously expressed at the mitochondria with critical anti–cell death function in immune and neuronal cells (14). These effects carry over into the heart, where HAX-1 can regulate cell death through endoplasmic reticulum stress (15) and mitochondrial stability (16) in myocardial ischemia reperfusion injury. In cardiomyocytes, HAX-1 also localizes to SR in addition to its ubiquitous mitochondrial localization, where it interacts with PLN (13) via AA 203–245 in HAX-1 and AA 16–22 in PLN (11). Phosphoryla-

This work was supported by National Institutes of Health Grants HL-26057 and HL-64018 (to E. G. K.) and HL-125204 (to P. A. B.) and American Heart Association Postdoctoral Fellowship 13POST13860006 (to P. A. B.). The authors declare that they have no conflicts of interest with the contents of this article. The content is solely the responsibility of the authors and does not necessarily represent the official views of the National Institutes of Health.

[1] To whom correspondence should be addressed. Tel.: 513-558-2377; Fax: 513-558-2269; E-mail: Litsa.Kranias@uc.edu.

[2] The abbreviations used are: SR, sarcoplasmic reticulum; SERCA2a, sarco/endoplasmic reticulum calcium ATPase 2a; PLN, phospholamban; AA, amino acid; HAXiKO, HAX-1 inducible knock-out; HAXOE, HAX-1 overexpression; PLNKO, phospholamban knock-out; PLNOE, PLN overexpression; RyR, ryanodine receptor; NCX, sodium/calcium exchanger; Hsp90, heat shock protein 90; ad.GFP, adenoviral GFP; ad.PLN, adenoviral PLN.

tion of PLN by protein kinase A during β-agonist stimulation results in dissociation of HAX-1 from PLN (11), suggesting a physiological relevance of this interaction. Previous work has shown that HAX-1 overexpression increases inhibition of SERCA2a by PLN and depresses contractility, whereas decreased expression of HAX-1 had the opposite effects (13, 15). Interestingly, loss of HAX-1 protein as a result of human mutations causes severe neutropenia, a rare immunodeficiency disease (14). In the mouse, global genetic deletion of HAX-1 associates with a short life span because of progressive loss of neuronal cells (14). Thus, the impact of HAX-1 deficiency in the heart and specifically on SERCA2a/PLN activity is not currently clear.

The present study was designed to delineate the role of endogenous HAX-1 on SR Ca^{2+} transport through the generation and characterization of a cardiac specific and inducible knock-out mouse model. We demonstrate for the first time that HAX-1 ablation relieves approximately 50% of the PLN inhibitory effects on SR Ca^{2+} transport, cardiomyocyte Ca^{2+} cycling, and contractile parameters. These findings suggest that endogenous HAX-1 is a critical regulator of PLN regulation and underline the significant function of this protein in the heart.

Results

Inducible HAX-1 ablation in the adult heart does not elicit compensatory changes in SR Ca^{2+}-handling proteins

Overexpression of HAX-1 in the heart has been shown to decrease Ca^{2+} cycling through increases in PLN inhibition, and these regulatory effects of HAX-1 are abrogated in the absence of PLN (13). Because global ablation of HAX-1 results in early lethality (17), we generated a cardiac-specific and inducible HAX-1 knock-out model (HAXiKO) to delineate the full contribution of endogenous HAX-1 in the heart. This was achieved by crossing a mouse with a floxed HAX-1 gene (17) with an α-myosin heavy chain mer-cre-mer transgenic mouse, which produces a cardiac specific cre recombinase activity upon tamoxifen treatment. Tamoxifen treatment was initiated at 2 months of age, and full cardiac ablation of HAX-1 was achieved after 14 days of tamoxifen (Fig. 1*A*). 14 days after termination of this treatment, we assessed the expression levels of SERCA2a, PLN, and ryanodine receptor (RyR). There were no differences between HAXiKO and WT hearts (Fig. 1, *A* and *B*). In addition, the levels of PLN phosphorylation at either Ser^{16} or Thr^{17} were similar (Fig. 1, *A* and *B*). These results indicate that any functional changes associated with HAX-1 ablation are not due to alteration of these SR Ca^{2+}-handling proteins.

Ablation of HAX-1 relieves 50% of PLN inhibition on cardiac contractile and Ca^{2+}-kinetic parameters

Overexpression of HAX-1 was previously shown to reduce cardiac contractility at the cellular level (13). To examine the function of endogenous HAX-1, cardiomyocytes were isolated from HAXiKO and WT mice, and contractile parameters were assessed by video edge detection (Fig. 2, *A–C*). It was observed that the fractional shortening and the rates of contraction and relaxation (+dL/dt and −dL/dt) were significantly increased in HAX-1–deficient cells, compared with WT controls (Fig. 2, *D–F*). In parallel studies, we included the PLNKO as an additional control, representing full relief of PLN inhibition and maximal SERCA2a activity (Fig. 2, *D–F*). The relative increases in the HAXiKO parameters were approximately half of those achieved in PLNKO cells. In addition, isoproterenol stimulation eliminated the differences between WT, HAXiKO, and

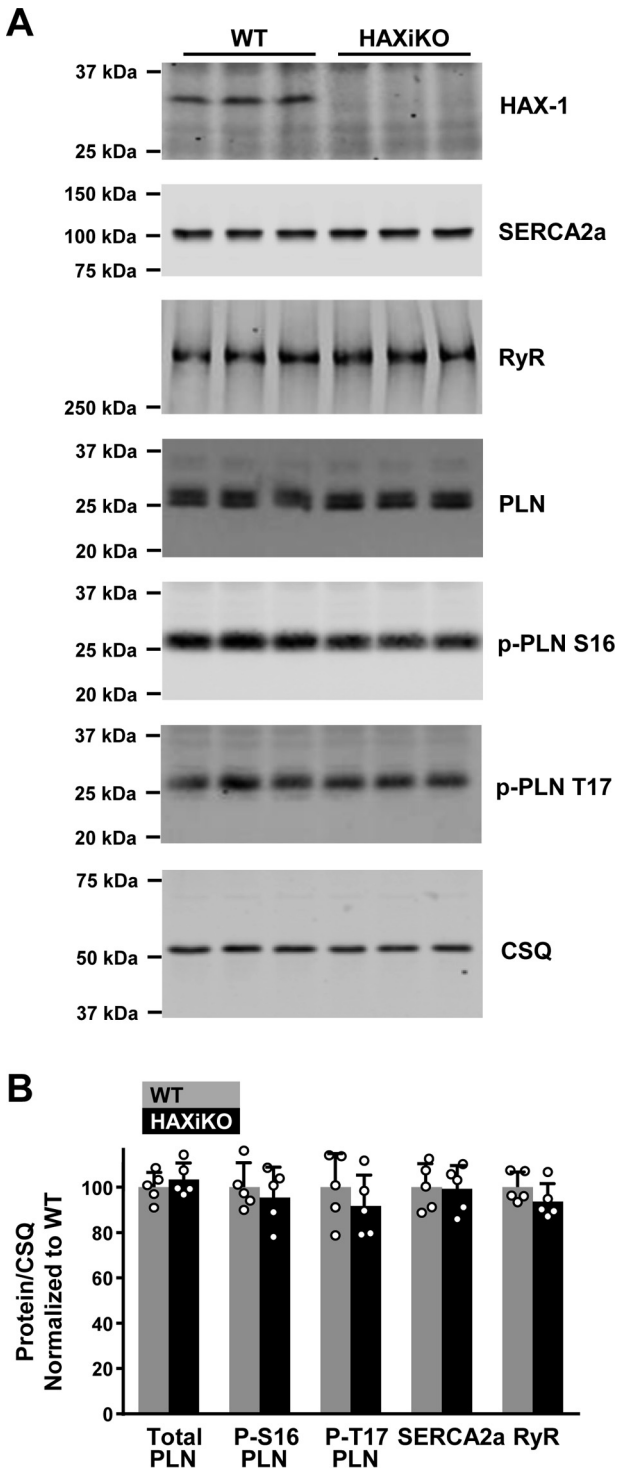

Figure 1. Cardiac-specific and inducible HAX-1 ablation does not alter Ca^{2+}-cycling protein levels. Representative Western blots from WT and HAXiKO heart homogenates (*A*) and corresponding quantitative analysis (*B*) show no changes in SERCA2a, RyR, and PLN protein levels or PLN phosphorylation status in response to inducible HAX-1 ablation in the adult heart (n = 5). The data are presented as the means ± S.D. *CSQ*, calsequestrin.

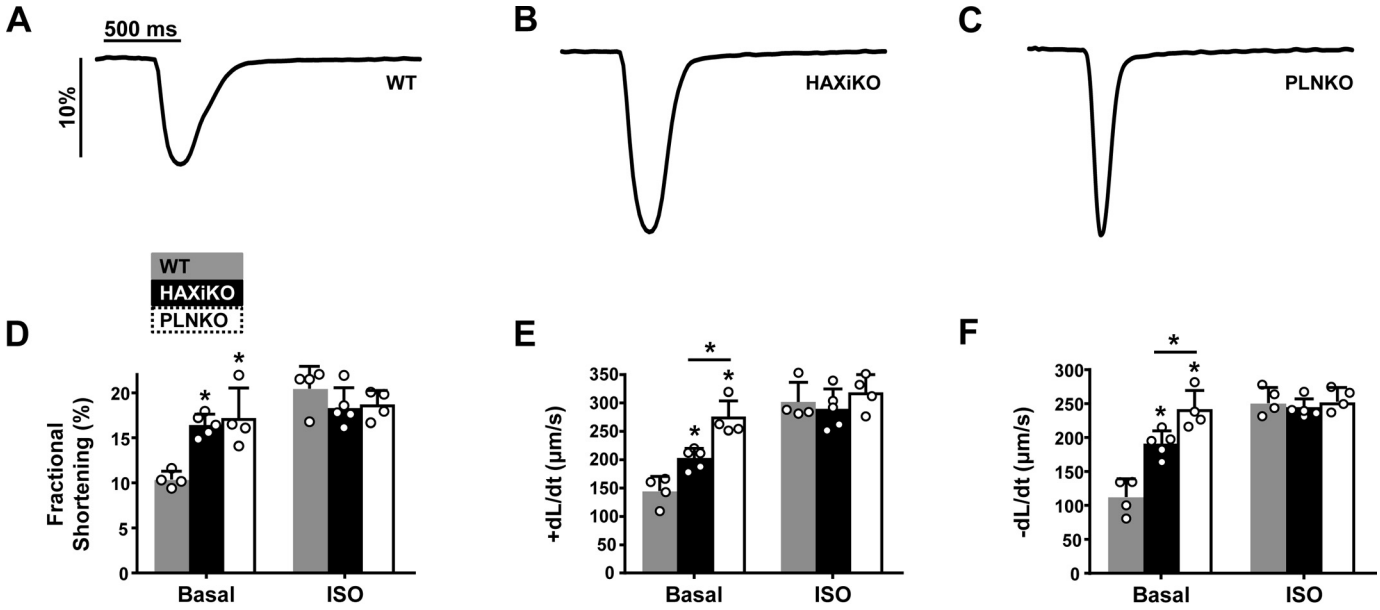

Figure 2. HAX-1 ablation increases cardiomyocyte contractile parameters. To determine the functional impact of HAX-1 ablation on the cellular level, cardiomyocytes were isolated from WT, HAXiKO, and PLNKO hearts, and contractile function was assessed by video edge detection at 0.5 Hz pacing under basal and isoproterenol (*ISO*) conditions. *A–C*, example cell length traces; *D*, fractional shortening; *E*, rate of contraction (+dL/dt); and *F*, rate of relaxation (−dL/dt) ($n = 4$ hearts, 8–10 cells/heart). The data are presented as the means ± S.D. *, $p < 0.05$ *versus* WT.

PLNKO, because the maximally stimulated contractile parameters were similar among these groups (Fig. 2, *D–F*), indicating that HAX-1 modulates function through PLN inhibition.

Ca^{2+} transient kinetics, measured in Fura-2 AM–loaded cardiomyocytes, were also consistent with the contractile parameters (Fig. 3, *A–C*). The transient amplitude was increased, and the decay time (T_{50}) and decay τ were shortened in HAXiKO cells, compared with WTs (Fig. 3, *D–F*). The observed changes in HAXiKO cardiomyocytes were approximately half of those achieved in PLNKO cells (Fig. 3, *D–F*). Isoproterenol stimulation also eliminated the differences between WT, HAXiKO, and PLNKO groups. The SR Ca^{2+} load, assessed by the caffeine-induced Ca^{2+}-peak, was higher in the HAXiKO cardiomyocytes (Fig. 3*G*). However, the decay rate of the caffeine-induced Ca^{2+} release was not altered, reflecting no alterations in Na/Ca^{2+} exchanger (NCX) activity (Fig. 3*H*). Furthermore, the increases in SR Ca^{2+} load by HAX-1 ablation were ~50% of those observed in PLNKO cells (Fig. 3*G*) without any differences in the decay time of the caffeine-induced Ca^{2+}-signal (Fig. 3*H*), indicating no alterations in NCX activity. These findings demonstrate that endogenous HAX-1 mediates ~50% of the PLN inhibitory effects in Ca^{2+} cycling and contractility in the cardiac myocytes.

HAX-1 deficiency increases the Ca^{2+} affinity of SERCA2a through decreased PLN binding

To determine whether the alterations in cardiomyocyte Ca^{2+} kinetics reflect alterations in SR Ca^{2+} transport, we assessed the effects of HAX-1 ablation on the initial rates of oxalate-supported SR Ca^{2+} uptake over a wide range of Ca^{2+} concentrations, similar to those present in the cardiomyocyte during relaxation and contraction (Fig. 4*A*). HAX-1 ablation resulted in significant increases in Ca^{2+}-transport rates but had no effect on the maximal velocity of the uptake system (WT, 80.1 ± 2.2 nmol/mg/min *versus* HAXiKO, 79.4 ± 2.8 nmol/mg/min, $n = 4$). Analysis of the EC_{50} value of Ca^{2+} transport for Ca^{2+} indicated that this parameter was decreased by 32% in the HAX-1 ablated hearts relative to WTs (Fig. 4*B*). In addition, PLN ablation resulted in 53% reduction of the EC_{50} (Fig. 4, *A* and *B*), suggesting that HAX-1 may mediate approximately half of the PLN inhibitory effects on SERCA2a activity. These alterations at the subcellular level reflect the increased functional parameters in cardiomyocytes (Figs. 2 and 3). The observed decrease in EC_{50} of HAX-1 knock-out hearts was not associated with changes in PLN levels or PLN phosphorylation (Fig. 1, *A* and *B*). To test whether HAX-1 ablation may alter the interaction between SERCA2a and PLN, WT, and HAXiKO, cardiac homogenates were subjected to co-immunoprecipitation experiments, using SERCA2a as bait. Indeed, HAX-1 ablation decreased the amount of PLN pulled down by SERCA2a (Fig. 4, *C* and *D*), consistent with reduced PLN inhibition and increased SR Ca^{2+}-uptake rates (Fig. 4, *A* and *B*).

Increased PLN expression does not alter contractile parameters in the absence of HAX-1

The observed decreased interaction between PLN and SERCA2a in the HAX-1 ablated hearts (Fig. 4, *C* and *D*) could be also attributed to lower affinity between these two proteins in the absence of HAX-1. In this case, increased PLN expression should be able to overcome the reduced binding and diminish the effects of HAX-1 ablation on the hypercontractile phenotype. To test this hypothesis, isolated cardiomyocytes from WT and HAXiKO mice were infected with either adenoviral GFP (ad.GFP) or PLN (ad.PLN), and the contractile parameters were then assessed. Overexpression of PLN in WT cells depressed fractional shortening, +dL/dt, and −dL/dt compared with ad.GFP control (Fig. 5, *A–C*). Interestingly, the depressed parameters were similar to those observed in cardiomyocytes

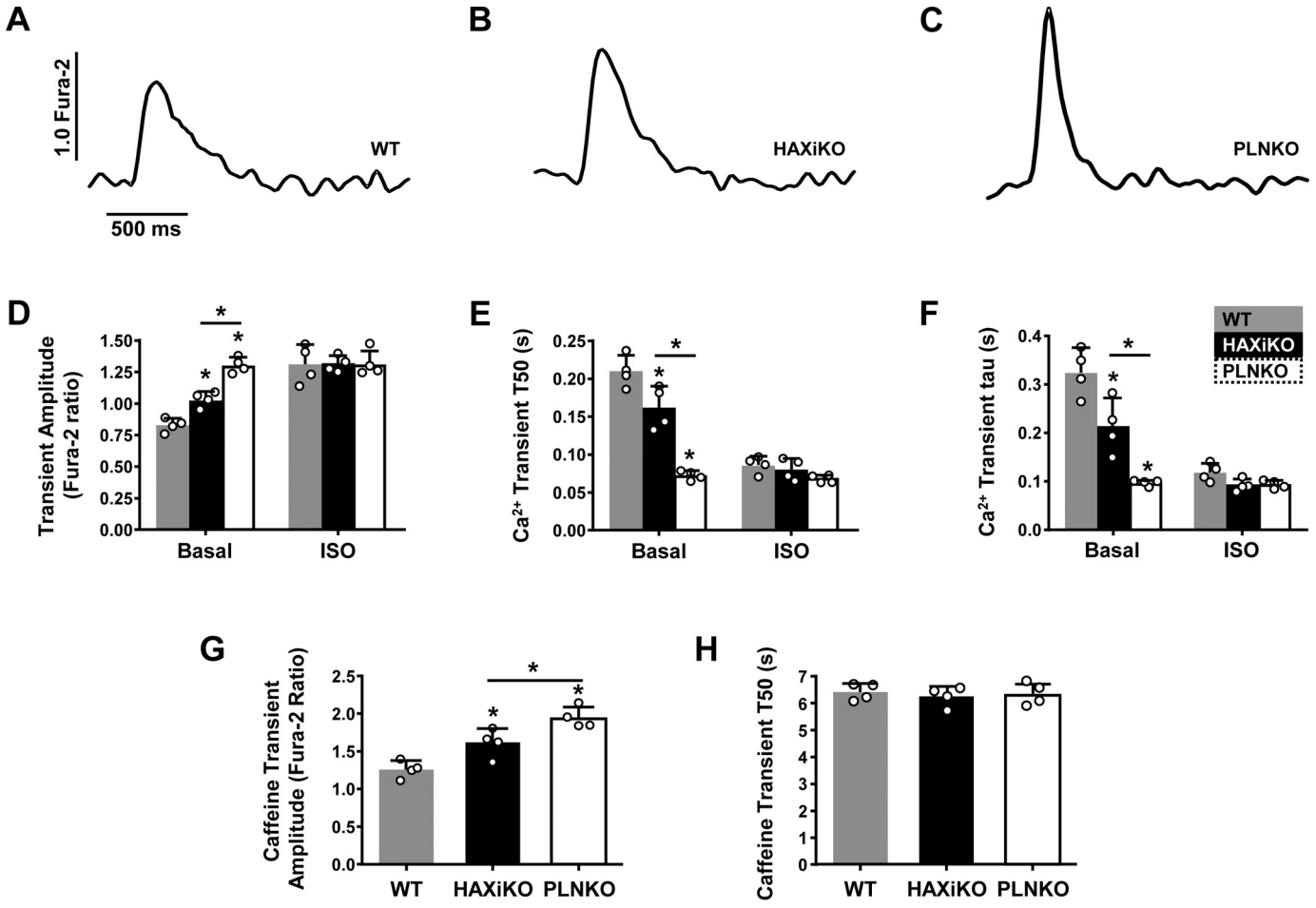

Figure 3. HAX-1 ablation increases cardiomyocyte Ca^{2+} transient parameters. To determine the impact of HAX-1 ablation on cellular Ca^{2+} kinetics, cardiomyocytes were isolated from WT, HAXiKO, and PLNKO hearts and loaded with Fura-2 AM and Ca^{2+} transients were assessed at 0. 5 Hz pacing under basal and isoproterenol (*ISO*) conditions. *A–C*, example Ca^{2+} transient traces; *D*, Ca^{2+} transient amplitude; *E*, time to 50% decay (T_{50}); and *F*, decay τ. *G* and *H*, SR Ca^{2+} load was also measured by the amplitude of caffeine induced Ca^{2+} transient (*G*) and NCX activity was determined by the decay (T_{50}) of caffeine induced transient (*H*) ($n = 4$ hearts, 8–10 cells/heart). The data are presented as the means ± S.D. *, $p < 0.05$ *versus* WT.

isolated from hearts with 2.5-fold overexpression of PLN (PLNOE), which we had previously observed to functionally saturate inhibition by PLN (9). However, PLN overexpression in HAXiKO cardiomyocytes had no effect on contractile parameters (Fig. 5, *A–C*). In parallel control experiments, PLN overexpression was also able to reduce function in HAXOE and PLNKO cells (Fig. 5, *A–C*). These results indicate that in the absence of HAX-1, endogenous levels of PLN have a functionally saturating effect on SR Ca^{2+} cycling and contractile parameters.

Discussion

This study presents the first evidence that endogenous HAX-1 mediates approximately half of the PLN inhibitory effects and serves as a gatekeeper for PLN activity in the heart. Elucidation of the functional role of HAX-1 is of paramount importance because human mutations have been identified that result in loss of this protein (8). The human carriers present with severe neutropenia (14), but the effects of HAX-1 ablation in cardiac function have not been determined. Furthermore, ablation of HAX-1 in the mouse results in early death caused by neurological defects (17), precluding assessment of its role in the heart. Thus, we generated an inducible and cardiac specific knock-out model to explicitly assess the *in vivo* function of HAX-1. Ablation of HAX-1 in the adult heart resulted in increased SERCA2a Ca^{2+} affinity and enhanced cardiomyocyte Ca^{2+} cycling and contractility. Importantly, the regulatory effects of HAX-1 were mediated through controlling the binding of PLN to SERCA2a and modulating PLN inhibition (Fig. 4, *C* and *D*, and Ref. 13). In fact, we observed that endogenous HAX-1 contributes to approximately 50% of the PLN inhibitory effects. There were no alterations on the maximal velocity of SERCA2a in HAX-1–deficient hearts, further supporting regulation of the transport system through PLN. These findings, combined with previous results in HAX-1 overexpression and HAX-1 heterozygous hearts (7), indicate that there is a close linear correlation (Fig. 6) between the relative changes of cardiomyocyte contraction rate ($-dL/dt$), Ca^{2+} transient T_{50}, and Ca^{2+} uptake EC_{50} against the HAX-1 expression levels (HAXiKO, HAXhet, WT, and HAXOE). Thus, HAX-1 is a critical component of the PLN·SERCA2a regulatory complex, and its levels have a significant impact in cardiomyocyte Ca^{2+} cycling and contractility. Decreased HAX-1 expression observed in disease states (15) may then represent a compensatory mechanism to boost cardiac function.

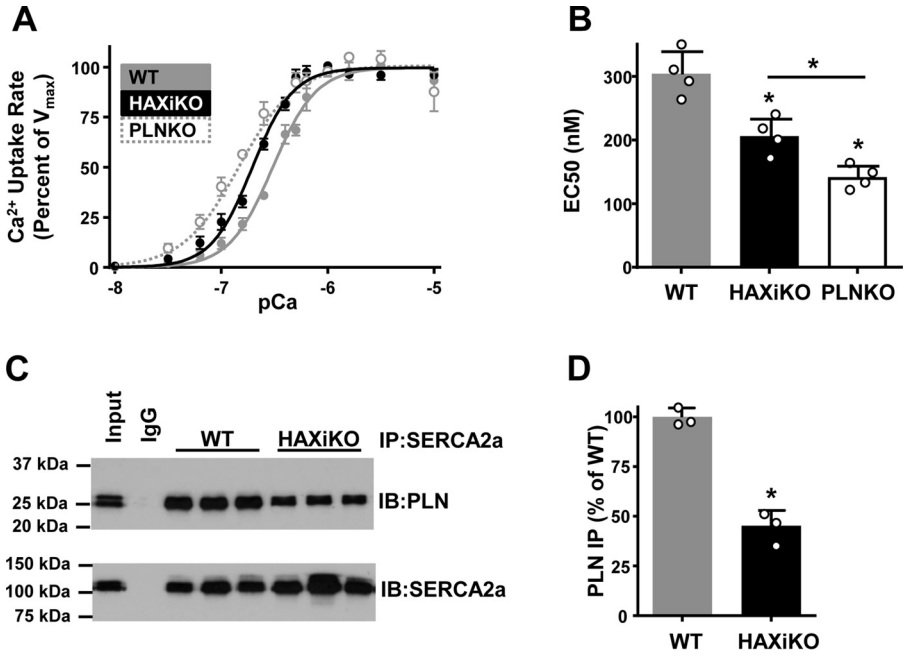

Figure 4. HAX-1 ablation enhances SR Ca^{2+} uptake rates and reduces PLN binding to SERCA2a. *A* and *B*, to determine the impact of HAX-1 on SERCA activity, we assessed the initial rates of oxalate-supported SR Ca^{2+} uptake in cardiac homogenates from WT, HAXiKO, and PLNKO mice (*A*) and the EC_{50} values of SERCA2a for Ca^{2+} (*B*). The values were normalized to maximal velocity (V_{max}) parameters ($n = 4$ hearts; each heart done in duplicate. *C*, representative Western blots for co-immunoprecipitation experiments using SERCA2a as bait and probing for PLN interaction. *D*, quantification of PLN pulled down by SERCA2a in WT and HAXiKO heart homogenates ($n = 3$). The data are presented as the means ± S.D. *, $p < 0.05$ *versus* WT. *IB*, immunoblot; *IP*, immunoprecipitation.

Previous studies reported that maximal inhibition of SERCA2a and cardiac contractility is achieved by 2.5-fold overexpression of PLN, suggesting that ~40% of SERCA2a activity is functionally inhibited by PLN in wild-type hearts (9). Consequently, the current results indicate that this fraction of inhibited SERCA2a by PLN could get further reduced to 20% in the absence of HAX-1 (Fig. 7*A*). In addition, our findings reveal that the previously reported maximal inhibition (PLNOE) of SERCA2a and contractility by PLN was restricted by endogenous levels of HAX-1. Indeed, dual overexpression of HAX-1 and PLN sets a new maximal "functional saturation level" of SERCA2a inhibition. Extrapolation from this new maximal inhibition to WT hearts suggests that ~30% of SERCA2a is functionally inhibited by PLN/HAX-1 under basal conditions (Fig. 7*B*). However, we must acknowledge that this estimate is limited by current knowledge and could be further modified through identification of additional regulatory factors.

The inability of PLN overexpression to diminish contractile parameters in the absence of HAX-1 (Fig. 5) demonstrates the nodal role of this protein in regulating the dynamic range of SERCA2a inhibition. This result also suggests that HAX-1 does not alter the binding affinity between PLN and SERCA2a. Further co-immunoprecipitation experiments would have provided additional information along these lines, but such studies are limited by the minimal lysate protein obtained from virally infected and cultured adult mouse cardiomyocytes. However, it is interesting to propose that our findings may reflect one or a combination of the following mechanisms: (*a*) HAX-1 may be necessary for displacing another unknown protein that modifies the PLN/SERCA2a interaction; (*b*) HAX-1 ablation may result in an unknown post-translational modification of SERCA2a, such that PLN regulation is functionally limited; and (*c*) PLN–SERCA2a regulation may involve functional units of either one PLN interacting with one SERCA2a molecule (18) or one PLN interacting with a SERCA2a dimer (19). Thus, if HAX-1 modulates the balance between these functional units, then ablation of HAX-1 may favor the dimeric complex (2 SERCA2a: 1 PLN) and potentially saturate regulation of SERCA2a with a lower abundance of PLN.

Interestingly, phosphorylation of PLN results in its dissociation from HAX-1 (11). As such, the inotropic and lusitropic effects of isoproterenol in the present study could be partially facilitated by loss of HAX-1 binding to PLN. In addition, the stimulatory effects of HAX-1 ablation may be partially attributed to loss of its co-chaperone protein Hsp90. Hsp90 was previously shown to interact with HAX-1 and facilitate its inhibitory effects on SR Ca^{2+} uptake (15). Thus, removal of HAX-1 may disrupt the compartmentalization of the HAX-1·Hsp90 complex, resulting in overall disinhibition of SERCA2a activity. Furthermore, several homologs of PLN have been identified (sarcolipin (20), myoregulin (21), DWORF (22), endoregulin (23), and another-regulin (23)) that regulate SERCA to varying degrees. However, these homologs do not contain AA residues 16–22 of PLN (11), which bind to HAX-1, and therefore may lack HAX-1 regulation. Nevertheless, it is intriguing to speculate that these PLN homologs may have their own undiscovered HAX-1 counterparts that are critical to their function.

In summary, the current study is the first to quantify the degree by which endogenous HAX-1 contributes to PLN inhibition and highlights HAX-1 as an important brake to control SERCA2a activity. Our findings also provide additional insights into the SERCA2a/PLN/HAX-1 regulatory axis and suggest that HAX-1 may be critical for amplification of the heart's

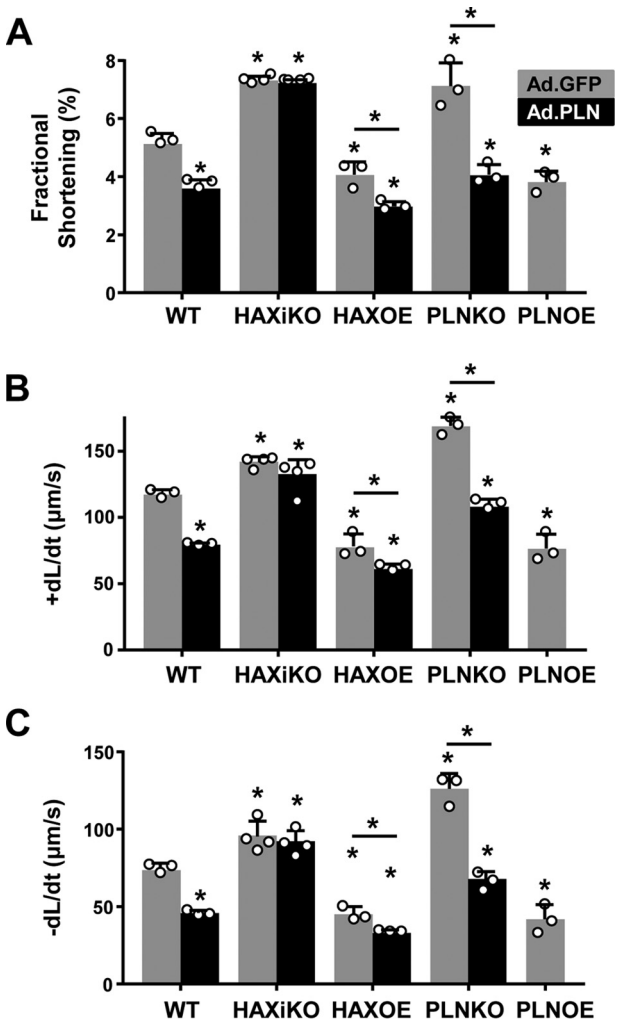

Figure 5. Increased PLN expression does not reverse the effects of HAX-1 ablation. To determine the impact of PLN overexpression in the absence of HAX-1, cardiomyocytes from WT, HAXiKO, HAXOE, and PLNKO hearts were isolated and infected with ad.GFP or ad.PLN. PLNOE cardiomyocytes were used as an additional control. 24 h after infection, contractile function was assessed by video edge detection and quantified by fractional shortening (*A*), rate of contraction (+dL/dt) (*B*), and rate of relaxation (−dL/dt) (*C*) ($n = 3–4$ hearts, 8–10 cells/heart). The data are presented as the means ± S.D. *, $p < 0.05$ *versus* WT.

responses to "flight or fight" situations as the heart strives to increase contractility and meet the demands of the periphery.

Experimental procedures

Animal models

HAX-1 inducible knock-out (HAXiKO) and their wild-type littermates were used in this study. HAXiKO mice were developed by crossing a floxed HAX-1 mouse (a gift from Dr. James Ihle, St. Jude, Memphis TN) with a transgenic mer/cre/mer containing the myosin heavy chain promoter (24). To induce cre recombinase activity and HAX-1 ablation, 8-week-old male mice were treated with tamoxifen (40 mg/kg) for 14 days. Experiments were performed on 12–14-week-old male mice, which was 2–4 weeks after termination of tamoxifen treatment. The mice were bred and maintained in the animal facility at the University of Cincinnati according to the institutional and the National Institutes of Health guidelines for animal care and use (publication no. 8523).

Western blot analysis

The snap-frozen hearts were suspended in cell lysis buffer (Cell Signaling) containing 1 mM PMSF, protease inhibitor (Roche Applied Science), and phosphatase inhibitors I and II (Calbiochem) and homogenized. For immunoblotting, 5–120 μg of protein was separated by SDS-PAGE gel electrophoresis using 6–12% polyacrylamide gels followed by electrotransfer to 0.1–0.45-μm nitrocellulose membranes. Blots were blocked in 5% milk and then probed overnight at 4 °C using the following primary antibodies: monoclonal HAX-1 (1:1000; BD Biosciences), monoclonal PLN (1:5000; Thermo Fisher), monoclonal RyR2 (1:1000; Thermo Fisher), and polyclonal calsequestrin (1:5000; Thermo Fisher). Licor fluorescent mouse or rabbit specific secondary antibodies were used at a dilution of 1:10,000 and visualized by using Licor Odyssey imager. All protein levels were quantified with the Licor Image Studio. For each protein, the densitometric values from WT controls were arbitrarily converted to 100%, and the values of samples from the other groups were normalized accordingly and expressed as a percentage of WT. Calsequestrin was used as an internal standard.

Mouse myocyte isolation and viral infection

Isolation of mouse left ventricular myocytes was carried out as described previously (16). Briefly, mouse hearts were excised from anesthetized (Euthasol, 200 mg/kg i.p.; Virbac AH, Inc.) adult mice, mounted in a Langendorff perfusion apparatus, and perfused with calcium-free Tyrode solution (140 mM NaCl, 4 mM KCl, 1 mM $MgCl_2$, 10 mM glucose, and 5 mM HEPES, pH 7.4.) at 37 °C for 3 min. Perfusion was then switched to the Tyrode solution containing liberase enzyme (0.25 mg/ml; Roche) for 8–15 min. The left ventricular tissue was excised, minced, pipette-dissociated, and filtered through a 240-μm screen. The cell suspension was then sequentially washed in 25, 100, and 200 μM and 1 mM Ca^{2+}-Tyrode, and resuspended in 1.8 mM Ca^{2+}-Tyrode for further experimentation.

For viral infection, freshly isolated myocytes were plated on laminin-coated coverslips (10 μg/ml) for 1 h at 5% CO_2 and 95% air at 37 °C. After the attachment, cardiac myocytes were transduced with adenoviruses to express either ad.PLN or ad.GFP at a multiplicity of infection of 500 and incubated for 3 h at 37 °C. Then medium was replaced with culture medium (DMEM containing 5 mg/liter ITS (bovine insulin, human transferrin and sodium selenite; Sigma), 100 units/ml penicillin streptomycin, 2 mM L-glutamine, 4 mM $NaHCO_3$, 10 mM HEPES, 0.2% BSA, and 25 μM blebbistatin (Cayman Chemical)). Experiments were performed 24 h after infection.

Measurements of mechanics and Ca^{2+} kinetics

Cell contractility and Ca^{2+} transients were measured at room temperature (22–23 °C) in separate experiments as previously described (13). Myocytes were field-stimulated to contract by a Grass S5 stimulator through platinum electrodes placed alongside the bath (0.5 Hz, bipolar pulses with

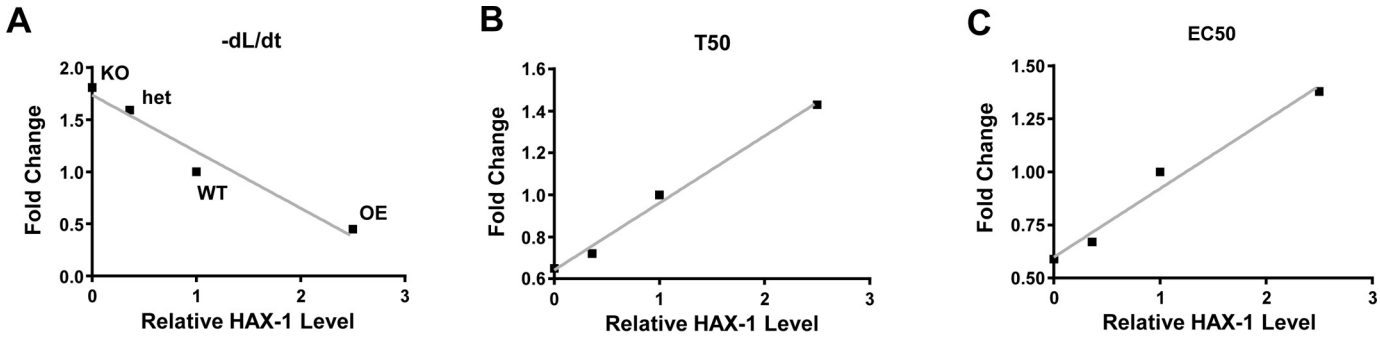

Figure 6. Functional parameters correlate with HAX-1 expression levels. Based on current and previously published data (13), the fold change in functional parameters from HAX-1 overexpression (*OE*), WT, HAX-1 heterozygous knock-out (*Het*), and HAXiKO (*KO*) samples were plotted against HAX-1 expression levels. *A*, rate of isolated cardiomyocyte relaxation (−dL/dt) measured by video edge detection; *B*, Ca^{2+} transient T_{50} measured from Fura-2 AM–loaded cardiomyocytes; and *C*, oxalate supported Ca^{2+} uptake EC_{50}. Linear regression for all plots yielded R^2 values greater than 0.95.

Figure 7. Schematic showing the relative functional inhibition of SERCA2a by PLN/HAX-1. *A*, an "old" scale based on previous data (9) using PLNOE as the reference point for maximal inhibition (100%), with PLNKO used as no inhibition (0%). *B*, new data suggest that dual overexpression of PLN with HAX-1 (PLNOE/HAXOE) inhibits SERCA2a more than PLNOE alone, which is used as the basis for a "new" maximal inhibition (100%) of SERCA2a. Based on the "old" scale, PLN was suggested to functionally inhibit 40% of SERCA2a in WT hearts (9). The "new" scale demonstrates that this functional inhibition of SERCA by PLN/HAX-1 is closer to 30% in WT hearts. This schematic also demonstrates that in the absence of HAX-1 (HAXiKO), PLN has a limited dynamic range of inhibition.

voltages 50% above myocyte voltage threshold). Contractions of myocytes from random fields were assessed by video edge detection. For Ca^{2+} transient measurements, the cells were loaded with Fura-2 (Fura-2 AM; 2 μM; Thermo Fisher) and alternately excited at 340 and 380 nm by a Delta Scan dual-beam spectrophotofluorometer (Photon Technology International) at baseline conditions and upon rapid application of 10 mM caffeine (Sigma). Calcium transients were expressed as the 340/380-nm ratio of the resulting 510-nm emissions. Rapid application of 10 mM caffeine was used to induce release of SR Ca^{2+} and assess the SR Ca^{2+} load, as well as obtain the participation of Na/Ca^{2+} exchange during $[Ca^{2+}]_i$ decline. The cells were superfused with normal Tyrode solution and stimulated at 0.5 Hz until twitch characteristics stabilized before each caffeine application. The amplitude of the caffeine-induced Ca^{2+} transients can be used as an index of SR Ca^{2+} content. Decline of $[Ca^{2+}]_i$ during a caffeine-induced Ca^{2+} transient in normal Tyrode was attributable to Na/Ca^{2+} exchange. Caffeine solution was introduced into the chamber and was continued for 20 s to study the kinetics of $[Ca^{2+}]_i$ decline. Measurements of mechanics and Ca^{2+} kinetics were also performed in the presence of isoproterenol 100 nM at 0.5 Hz. Contractility and transient data were analyzed by Felix software (Photon Technology International).

Oxalate supported Ca^{2+} uptake

Ca^{2+} uptake assays were performed as previously described (12, 13). Hearts from were frozen under liquid nitrogen and stored at −80 °C until processed. Frozen hearts were homogenized in 50 mM KH_2PO_4, pH 7.0, 10 mM NaF, 1 mM EDTA, 0.3 M sucrose, 0.3 mM phenylmethylsulfonyl fluoride, and 0.5 mM dithiothreitol. Ca^{2+} uptake in whole-heart homogenates (0.1 mg/ml) was measured by a modification of the Millipore filtration technique. The reaction contained 40 mM imidazole, pH 7.0, 100 mM KCl, 5 mM $MgCl_2$, 5 mM NaN_3, 5 mM potassium oxalate, 0.5 mM EGTA, 1, μM ruthenium red, and various concentrations of $CaCl_2$ to yield 0.02 to 5 μM free

Ca^{2+}. Homogenates were incubated at 37 °C for 2 min in the above buffer, and the reaction was initiated by the addition of ATP (final concentration, 5 mM). The rates of Ca^{2+} uptake were calculated by least squares linear regression analysis of 30-, 60-, and 90-s time points. The data were analyzed by nonlinear regression using ORIGIN (version 6.0) software.

Co-immunoprecipitations

Co-immunoprecipitations were performed as previously described (15). Briefly, hearts were homogenized with 1× cell lysis buffer (Cell Signaling Technology) supplemented with protease inhibitor mixture and phosphatase inhibitor mixture and was diluted to 1 mg/ml and incubated with anti-SERCA2a (BD Biosciences) or IgG antibody (Santa Cruz Biotechnology) at 4 °C overnight with rotation. Protein G Plus-agarose beads (Santa Cruz Biotechnology) were added into the mixture and incubated for an additional 5 h, sedimented, and washed six times with the cell lysis buffer. Bead-bound proteins were dissociated in 2× SDS and probed by Western blots. WT heart homogenate was used as positive control (input), and immunoprecipitate with anti-IgG Plus-agarose was used as negative control (IgG).

Statistical analysis

The data were expressed as the means ± S.D. Comparisons between the means of two groups were performed by unpaired Student's *t* test. Multiple groups were analyzed by using two-way analysis of variance followed by Tukey's multiple comparisons. The results were considered statistically significant at $p < 0.05$.

Author contributions—P. A. B. and E. G. K. conceptualization; P. A. B. and K. H. data curation; P. A. B. and K. H. formal analysis; P. A. B. and K. H. investigation; P. A. B. methodology; P. A. B. writing-original draft; P. A. B. and E. G. K. writing-review and editing; E. G. K. supervision; E. G. K. project administration.

Acknowledgments—We thank Dr. James Ihle and Dr. Evan Parganas (St. Jude, Memphis TN) for graciously donating the floxed HAX-1 mouse.

References

1. Kranias, E. G., and Hajjar, R. J. (2012) Modulation of cardiac contractility by the phospholamban/SERCA2a regulatome. *Circ. Res.* **110,** 1646–1660 CrossRef Medline
2. Zima, A. V., Bovo, E., Mazurek, S. R., Rochira, J. A., Li, W., and Terentyev, D. (2014) Ca handling during excitation-contraction coupling in heart failure. *Pflugers Arch.* **466,** 1129–1137 CrossRef Medline
3. MacLennan, D. H., and Kranias, E. G. (2003) Phospholamban: a crucial regulator of cardiac contractility. *Nat. Rev. Mol. Cell Biol.* **4,** 566–577 CrossRef Medline
4. Traaseth, N. J., Ha, K. N., Verardi, R., Shi, L., Buffy, J. J., Masterson, L. R., and Veglia, G. (2008) Structural and dynamic basis of phospholamban and sarcolipin inhibition of Ca $^{2+}$-ATPase. *Biochemistry* **47,** 3–13 CrossRef Medline
5. Luo, W., Grupp, I. L., Harrer, J., Ponniah, S., Grupp, G., Duffy, J. J., Doetschman, T., and Kranias, E. G. (1994) Targeted ablation of the phospholamban gene is associated with markedly enhanced myocardial contractility and loss of β-agonist stimulation. *Circ. Res.* **75,** 401–409 CrossRef Medline
6. Wolska, B. M., Stojanovic, M. O., Luo, W., Kranias, E. G., and Solaro, R. J. (1996) Effect of ablation of phospholamban on dynamics of cardiac myocyte contraction and intracellular Ca^{2+}. *Am. J. Physiol.* **271,** C391–C397 Medline
7. Slack, J. P., Grupp, I. L., Dash, R., Holder, D., Schmidt, A., Gerst, M. J., Tamura, T., Tilgmann, C., James, P. F., Johnson, R., Gerdes, A. M., and Kranias, E. G. (2001) The enhanced contractility of the phospholamban-deficient mouse heart persists with aging. *J. Mol. Cell. Cardiol.* **33,** 1031–1040 CrossRef Medline
8. Kadambi, V. J., Ponniah, S., Harrer, J. M., Hoit, B. D., Dorn, G. W., 2nd, Walsh, R. A., and Kranias, E. G. (1996) Cardiac-specific overexpression of phospholamban alters calcium kinetics and resultant cardiomyocyte mechanics in transgenic mice. *J. Clin. Invest.* **97,** 533–539 CrossRef Medline
9. Brittsan, A. G., Carr, A. N., Schmidt, A. G., and Kranias, E. G. (2000) Maximal inhibition of SERCA2 Ca^{2+} affinity by phospholamban in transgenic hearts overexpressing a non-phosphorylatable form of phospholamban. *J. Biol. Chem.* **275,** 12129–12135 CrossRef Medline
10. Haghighi, K., Bidwell, P., and Kranias, E. G. (2014) Phospholamban interactome in cardiac contractility and survival: a new vision of an old friend. *J. Mol. Cell. Cardiol.* **77,** 160–167 CrossRef Medline
11. Vafiadaki, E., Sanoudou, D., Arvanitis, D. A., Catino, D. H., Kranias, E. G., and Kontrogianni-Konstantopoulos, A. (2007) Phospholamban interacts with HAX-1, a mitochondrial protein with anti-apoptotic function. *J. Mol. Biol.* **367,** 65–79 CrossRef Medline
12. Bidwell, P. A., and Kranias, E. G. (2016) Calcium uptake in crude tissue preparation. *Methods Mol. Biol.* **1377,** 161–170 CrossRef Medline
13. Zhao, W., Waggoner, J. R., Zhang, Z.-G., Lam, C. K., Han, P., Qian, J., Schroder, P. M., Mitton, B., Kontrogianni-Konstantopoulos, A., Robia, S. L., and Kranias, E. G. (2009) The anti-apoptotic protein HAX-1 is a regulator of cardiac function. *Proc. Natl. Acad. Sci. U.S.A.* **106,** 20776–20781 CrossRef Medline
14. Fadeel, B., and Grzybowska, E. (2009) HAX-1: a multifunctional protein with emerging roles in human disease. *Biochim. Biophys. Acta* **1790,** 1139–1148 CrossRef Medline
15. Lam, C. K., Zhao, W., Cai, W., Vafiadaki, E., Florea, S. M., Ren, X., Liu, Y., Robbins, N., Zhang, Z., Zhou, X., Jiang, M., Rubinstein, J., Jones, W. K., and Kranias, E. G. (2013) Novel role of HAX-1 in ischemic injury protection involvement of heat shock protein 90. *Circ. Res.* **112,** 79–89 CrossRef Medline
16. Lam, C. K., Zhao, W., Liu, G.-S., Cai, W.-F., Gardner, G., Adly, G., and Kranias, E. G. (2015) HAX-1 regulates cyclophilin-D levels and mitochondria permeability transition pore in the heart. *Proc. Natl. Acad. Sci. U.S.A.* **112,** E6466–E6475 CrossRef Medline
17. Chao, J.-R., Parganas, E., Boyd, K., Hong, C. Y., Opferman, J. T., and Ihle, J. N. (2008) Hax1-mediated processing of HtrA2 by Parl allows survival of lymphocytes and neurons. *Nature* **452,** 98–102 CrossRef Medline
18. Mueller, B., Karim, C. B., Negrashov, I. V., Kutchai, H., and Thomas, D. D. (2004) Direct detection of phospholamban and sarcoplasmic reticulum Ca-ATPase interaction in membranes using fluorescence resonance energy transfer. *Biochemistry* **43,** 8754–8765 CrossRef Medline
19. Blackwell, D. J., Zak, T. J., and Robia, S. L. (2016) Cardiac calcium ATPase dimerization measured by cross-linking and fluorescence energy transfer. *Biophys. J.* **111,** 1192–1202 CrossRef Medline
20. Wawrzynow, A., Theibert, J. L., Murphy, C., Jona, I., Martonosi, A., and Collins, J. H. (1992) Sarcolipin, the "proteolipid" of skeletal muscle sarcoplasmic reticulum, is a unique, amphipathic, 31-residue peptide. *Arch. Biochem. Biophys.* **298,** 620–623 CrossRef Medline
21. Anderson, D. M., Anderson, K. M., Chang, C.-L., Makarewich, C. A., Nelson, B. R., McAnally, J. R., Kasaragod, P., Shelton, J. M., Liou, J., Bassel-Duby, R., and Olson, E. N. (2015) A micropeptide encoded by a putative long noncoding RNA regulates muscle performance. *Cell* **160,** 595–606 CrossRef Medline
22. Nelson, B. R., Makarewich, C. A., Anderson, D. M., Winders, B. R., Troupes, C. D., Wu, F., Reese, A. L., McAnally, J. R., Chen, X., Kavalali,

E. T., Cannon, S. C., Houser, S. R., Bassel-Duby, R., and Olson, E. N. (2016) A peptide encoded by a transcript annotated as long noncoding RNA enhances SERCA activity in muscle. *Science* **351,** 271–275 CrossRef Medline

23. Anderson, D. M., Makarewich, C. A., Anderson, K. M., Shelton, J. M., Bezprozvannaya, S., Bassel-Duby, R., and Olson, E. N. (2016) Widespread control of calcium signaling by a family of SERCA-inhibiting micropeptides. *Sci. Signal.* **9,** ra119–ra119 CrossRef Medline
24. Sohal, D. S., Nghiem, M., Crackower, M. A., Witt, S. A., Kimball, T. R., Tymitz, K. M., Penninger, J. M., and Molkentin, J. D. (2001) Temporally regulated and tissue-specific gene manipulations in the adult and embryonic heart using a tamoxifen-inducible Cre protein. *Circ. Res.* **89,** 20–25 CrossRef Medline